$CuClSe_{1.53}Te_{0.47}$ and $CuClSe_{0.56}Te_{1.44}$: Structural and Vibrational Spectroscopic Investigations on Copper(I) Chalcogen Chlorides

Tom Nilges, Stefan Zimmerer, Daniel Kurowski, Arno Pfitzner*

Regensburg, Institut für Anorganische Chemie der Universität

Received July 16th, 2002

Dedicated to Professor Rudolf Hoppe on the Occasion of his 80th Birthday

Abstract. $CuClSe_{1.53}Te_{0.47}$ and $CuClSe_{0.56}Te_{1.44}$ are obtained from the reaction of CuCl, Se, and Te in stoichiometric amounts. Both copper(I) selenium tellurium chlorides are monoclinic, space group $P2_1/n$ (no. 14) with lattice constants of a = 7.837(1) Å, b = 4.699(1) Å, c = 10.762(2) Å, β = 104.37(2)°, V = 383.9(1) Å^3 ($CuClSe_{1.53}Te_{0.47}$), and a = 8.074(1) Å, b = 4.830(1) Å, c = 10.973(1) Å, β = 103.87(2)°, V = 415.5(1) Å^3 ($CuClSe_{0.56}Te_{1.44}$), and Z = 4. A common feature of these isostructural compounds are heteroatomic strands $^1_\infty$[YY'] (Y, Y' = chalcogen). These strands are running along [010] and are connected to layers by chains $^1_\infty$[CuCl]. Vibrational spectra of $CuClSe_{1.53}Te_{0.47}$, $CuClSe_{0.56}Te_{1.44}$, $CuXTe_2$ and $CuX'Se_2$ (X = Cl, Br, I; X' = Cl, Br) are analysed with respect to the bonding relations of the chalcogen chains. Modes derived from IR and Raman spectra are assigned by correlation with trigonal Se and related copper(I) chalcogen halides.

Both, X-ray structural data and an analysis of the chalcogen vibrational modes in IR and Raman spectra, lead to a detailed insight into the ordering phenomena of the chalcogen chains in this type of copper(I) chalcogen halides.

Keywords: Copper(I) chalcogen halides; Chalcogen chains; Crystal structure; IR spectroscopy; Raman spectroscopy

$CuClSe_{1.53}Te_{0.47}$ und $CuClSe_{0.56}Te_{1.44}$: Strukturelle und schwingungsspektroskopische Untersuchungen an Kupfer(I)-chalkogenchloriden

Inhaltsübersicht. $CuClSe_{1.53}Te_{0.47}$ und $CuClSe_{0.56}Te_{1.44}$ wurden durch Umsetzung von CuCl, Se und Te in stöchiometrischen Mengen erhalten. Beide Verbindungen kristallisieren monoklin, Raumgruppe $P2_1/n$ (Nr. 14) mit den Gitterkonstanten a = 7.837(1) Å, b = 4.699(1) Å, c = 10.762(2) Å, β = 104.37(2)°, V = 383.9(1) Å^3 ($CuClSe_{1.53}Te_{0.47}$) und a = 8.074(1) Å, b = 4.830(1) Å, c = 10.973(1) Å, β = 103.87(2)°, V = 415.5(1) Å^3 ($CuClSe_{0.56}Te_{1.44}$) und Z = 4. Gemeinsames Merkmal der isostrukturell kristallisierenden Verbindungen sind Ketten $^1_\infty$[YY'] (Y, Y' = Chalkogen). Die Chalkogenketten verlaufen parallel [010] und werden durch $^1_\infty$[CuCl]-Stränge zu Schichten verknüpft. IR- und Ramanspektren von $CuClSe_{1.53}Te_{0.47}$, $CuClSe_{0.56}Te_{1.44}$, $CuXTe_2$ und $CuX'Se_2$ (X = Cl, Br, I; X' = Cl, Br) wurden im Hinblick auf die Bindungseigenschaften der Chalkogenketten untersucht. Die Zuordnung der Moden erfolgte auf Basis der Spektren von trigonalem Se und verwandten Kupfer(I)-chalkogenhalogeniden.

Durch Kombination einer Besetzungsfaktoranalyse aus Einkristallstrukturdaten und der Auswertung der schwingungsspektroskopischen Daten, insbesondere der Moden der Chalkogenketten, werden die Ordnungsvarianten der Chalkogenketten der untersuchten Kupfer(I)-chalkogenhalogenide analysiert.

Introduction

Copper(I) halides have been established as a preparative tool giving access to neutral or low charged molecules and polymeric units of the 15th and 16th group of the PSE [1]. Starting in 1969 [2] several compounds of $^1_\infty$[Y]-chalcogen chains embedded in copper(I) halides have been characterized. Examples are $CuXSe_2$ (X = Cl, Br) [3, 4], $CuXTe_2$ (X = Cl, Br, I) [5, 6] and CuXTe [7-9]. Tellurium atoms in $CuXTe_2$ can be substituted in an ordered manner by sulphur or by selenium forming heteroatomic chains $^1_\infty$[STe], and $^1_\infty$[SeTe], respectively. The resulting compounds are CuXSTe (X = Cl, Br) [10], and CuXSeTe (X = Cl, Br, I) [11]. $CuXY_2$ and CuXY'Te (Y = Se, Te, Y' = S, Se) are isostructural and crystallise in space group $P2_1/n$ (no. 14). They consist of characteristic one-dimensional screw-like chalcogen strands and $^1_\infty$[CuX] chains directing along the b axis. Heteroatomic chains consisting of sulphur and selenium embedded in a copper halide are not yet known, but only six-membered rings $(S/Se)_6$ in $(CuX)_2(S/Se)_6$ (X = Br, I) [12]. Inorganic copper(I) halide substructures like Cu_2X_2 dimers, zigzag, single or staircase double chains are known as spacers to coordinate organic molecules [13], and are not

---

* Prof. Dr. A. Pfitzner
Institut für Anorganische Chemie
Universität Regensburg
D-93040 Regensburg
Fax: +49 941 943 4983
E-mail: arno.pfitzner@chemie.uni-regensburg.de

0044−2313/02/628/2809−2814 $ 20.00+.50/0

restricted to inorganic coordination compounds. These coordination polymers open up a promising new field of research.

Mixed Se_xTe_{1-x} chains can be stabilised in mordenite with a randomly mixed distribution of Se and Te [14]. Physical properties and bond distances of heteroatomic helical chains Se-Te of different composition were calculated by semi-empirical methods [15].

Spectroscopic investigations were reported for $CuBrSe_2$ [4], $(CuBr)_2Se_6$, and $(CuI)_2Se_6$ [16]. It became evident that the intermolecular chalcogen interactions are drastically reduced by the copper(I) halides. Therefore the copper halides might be regarded as a matrix for the chalcogen units. IR and Raman spectroscopy are useful tools to investigate the bonding situation within this type of compounds.

Two distinct crystallographic chalcogen positions are observed in the ternary copper(I) chalcogen halides $CuXY_2$. A pronounced ordered distribution of the different chalcogen atoms on these two positions is found in the case of quaternary copper(I) chalcogen halides CuXYY' with a chalcogen ratio of 1:1. Almost perfectly ordered heteroatomic chalcogen chains $^1_\infty$[YY'] result. The next step is to examine the substitution pattern for the chalcogen ratios of 3:1 and 1:3, and to get some insight into the ordering schemes. Single crystal X-ray structure analysis and spectroscopic methods are a useful combination of methods to investigate the resulting compounds.

Herein, we report the crystal structures of $CuClSe_{1.53}Te_{0.47}$ and $CuClSe_{0.56}Te_{1.44}$, and vibrational spectroscopic properties of $CuClSe_{1.53}Te_{0.47}$, $CuClSe_{0.56}Te_{1.44}$, $CuXTe_2$, and $CuX'Se_2$ (X = Cl, Br, I; X' = Cl, Br).

Results

Structure description and discussion

$CuClSe_{1.53}Te_{0.47}$ and $CuClSe_{0.56}Te_{1.44}$ crystallise monoclinic, space group $P2_1/n$ (no. 14) with lattice constants of a = 7.837(1) Å, b = 4.699(1) Å, c = 10.762(2) Å, β = 104.37(2)°, and V = 383.9(1) Å^3 ($CuClSe_{1.53}Te_{0.47}$), and a = 8.074(1) Å, b = 4.830(1) Å, c = 10.973(1) Å, β = 103.87(2)°, and V = 415.5(1) Å^3 ($CuClSe_{0.56}Te_{1.44}$). Z is 4 for both compounds. They are isostructural to the above mentioned ternary and quaternary copper(I) chalcogen halides $CuXY_2$ and CuXYY'. Crystallographic data, atomic positions, isotropic and anisotropic displacement parameters, and selected distances and angles are summarised in Tables 1−4.

The title compounds consist of chains, both of chalcogen atoms and of copper chloride. These chains run parallel [010]. Layers parallel (001) are formed by combination of left handed chalcogen chains with right handed copper chloride chains and vice versa. These layers are stacked along [001] and the orientation of the chains is reversed in every other layer. The attraction of Cl^- and positively polarized chalcogen atoms on the Y2 position can be regarded as the main interaction between the layers, see Figure 1. Copper is coordinated by chalcogen atoms and chloride ions forming $[CuY1Y2Cl_{2/2}]$ tetrahedra. Vertex sharing $[CuY1Y2Cl_{2/2}]$ tetrahedra extend along [010]. The angle τ (Cl−Cl−Cl) defined by the Cl atoms of two tetrahedra varies with the substitution of Te by Se and vice versa, see Figure 2. The chalcogen atoms tend to form heteroatomic bonds which can of course only be realized for the minority

Table 1 Selected crystallographic data of $CuClSe_{1.53}Te_{0.47}$ and $CuClSe_{0.56}Te_{1.44}$.

Compound	$CuClSe_{1.53}Te_{0.47}$	$CuClSe_{0.56}Te_{1.44}$
Formula weight/g mol^{-1}	281.23	329.87
Crystal size/mm^3	0.32 x 0.06 x 0.04	0.28 x 0.06 x 0.05
Color	silver	
Morphology	needles	
Crystal system	monoclinic	
Space group	$P2_1/n$ (no. 14)	
Lattice constants/Å	a = 7.837(1) b = 4.699(1) c = 10.762(2) β = 104.37(2)°	a = 8.074(1) b = 4.830(1) c = 10.973(1) β = 103.87(2)°
Cell volume, Z	383.9(1), 4	415.5(1), 4
$\rho_{X\text{-}ray}$/g cm^{-3}	4.866	5.274
μ/mm^{-1}	24.07	20.37
Diffractometer	STOE IPDS MoK_α, λ = 0.71073 Å, oriented graphite monochromator	
Image plate distance/mm	60	
φ-range/°, $\Delta\varphi$/°	$1 \leq \varphi \leq 359.2$, 1.8	$0 \leq \varphi \leq 360$, 1.8
Temperature/K	293	
θ-range/°	$2.90 < \theta < 28.01$	$2.83 < \theta < 28.05$
hkl-range	$-10 \leq h \leq 10$ $-5 \leq k \leq 5$ $-14 \leq l \leq 14$	$-10 \leq h \leq 10$ $-6 \leq k \leq 6$ $-14 \leq l \leq 14$
No. of reflections, $R_{int.}$	6302; 0.0664	6931; 0.0352
No. of independent reflections	890	1001
No. of parameters	39	39
Program	SHELXL97 [23]	
$R(I>2\sigma(I))$, R (all reflections)	0.0173; 0.0252	0.0276, 0.0276
$wR(I>2\sigma(I))$, wR (all reflections)	0.0329; 0.0339	0.0652, 0.0657
GooF	0.863	1.018
Largest difference peaks $\Delta\rho_{min}$, $\Delta\rho_{max}$/e Å^{-3}	−0.487, 0.563	−1.287, 1.600

Further details of the crystal structure investigations are available from the Fachinformationszentrum Karlsruhe, D-76344 Eggenstein-Leopoldshafen (Germany), Fax: 0049 7247 808 666, E-mail: crysdata@fiz-karlsruhe.de, on quoting the depository number CSD-412714 ($CuClSe_{0.56}Te_{1.44}$) and CSD-412715 ($CuClSe_{1.53}Te_{0.47}$), name of the authors and reference.

Table 2 Atomic coordinates and isotropic displacement parameters in Å^2 of $CuClSe_{1.53}Te_{0.47}$ and $CuClSe_{0.56}Te_{1.44}$.

Atom	x	y	z	sof	U_{eq}*
$CuClSe_{1.53}Te_{0.47}$					
Cu	0.42480(5)	0.1361(1)	0.25174(6)	1.0	0.0281(2)
Cl	0.7026(1)	0.1215(2)	0.6103(1)	1.0	0.0241(2)
Y(1)	0.42286(4)	0.21828(8)	0.84754(4)	0.073(2) (Te) 0.927 (Se)	0.0207(1)
Y(2)	0.85481(3)	0.00038(7)	0.14382(3)	0.400(2) (Te) 0.600 (Se)	0.02190(1)
$CuClSe_{0.56}Te_{1.44}$					
Cu	0.42381(7)	0.1376(1)	0.25150(6)	1.0	0.0305(2)
Cl	0.7055(1)	0.1217(3)	0.6158(1)	1.0	0.0264(3)
Y(1)	0.43302(4)	0.22078(8)	0.85598(3)	0.501(3) (Te) 0.499	0.0244(2) (Se)
Y(2)	0.86209(3)	0.00171(6)	0.13696(3)	0.944(3) (Te) 0.056	0.0220(1) (Se)

* U_{eq} is defined as one third of the trace of the orthogonalized U_{ij} tensor.

Table 3 Anisotropic displacement parameters in Å^2 of $CuClSe_{1.53}Te_{0.47}$ and $CuClSe_{0.56}Te_{1.44}$.

Atom	U_{11}	U_{22}	U_{33}	U_{23}	U_{13}	U_{12}
$CuClSe_{1.53}Te_{0.47}$						
Cu	0.0167(2)	0.0285(4)	0.0396(4)	0.0047(2)	0.0081(2)	0.0006(2)
Cl	0.0187(3)	0.0299(6)	0.0235(5)	0.0005(4)	0.0049(3)	0.0065(3)
Y(1)	0.0150(1)	0.0223(2)	0.0249(2)	0.0008(2)	0.0052(1)	0.007(1)
Y(2)	0.0148(1)	0.0203(2)	0.0298(2)	0.0020(1)	0.0042(1)	0.0003(1)
$CuClSe_{0.56}Te_{1.44}$						
Cu	0.0204(3)	0.0305(4)	0.0416(4)	0.0022(3)	0.0096(2)	0.0010(2)
Cl	0.0209(5)	0.0313(7)	0.0273(5)	0.0019(4)	0.0064(4)	0.0049(4)
Y(1)	0.0178(2)	0.0256(2)	0.0312(2)	0.0041(1)	0.0088(1)	0.0007(1)
Y(2)	0.0178(2)	0.0229(2)	0.0257(2)	0.0003(1)	0.0060(1)	0.00102(9)

Table 4 Selected interatomic distances in Å and angles in degrees of $CuClSe_{1.53}Te_{0.47}$ and $CuClSe_{0.56}Te_{1.44}$.

	$CuClSe_{1.53}Te_{0.47}$	$CuClSe_{0.56}Te_{1.44}$
$Y1-Y2^a$	2.427(2)	2.632(1)
$Y1-Y2^b$	2.504(9)	2.691(7)
$Y1-Cu^a$	2.445(1)	2.525(8)
$Y2-Cu^c$	2.491(2)	2.563(1)
$Cl-Cu^a$	2.326(1)	2.348(1)
$Cl-Cu^e$	2.310(2)	2.329(2)
$Y1^a-Y2-Y1^d$	100.83(2)	100.22(1)
$Y2^a-Y1-Y2^b$	104.99(2)	103.26(2)
$Y1^a-Y2-Cu^c$	102.79(2)	102.57(2)
$Y2^a-Y1-Cu^a$	105.61(2)	104.65(2)
$Cu^a-Y1-Y2^b$	89.94(2)	86.99(2)
$Cu^c-Y2-Y1^d$	89.70(2)	86.59(2)
$Y1^a-Cu-Y2^g$	107.78(2)	111.20(3)
$Cl^a-Cu-Y1^a$	104.97(3)	104.21(4)
$Cl^f-Cu-Y1^a$	114.71(3)	113.89(4)
$Cl^f-Cu-Y2^g$	106.53(3)	106.47(4)
$Cl^a-Cu-Y2^g$	115.38(3)	114.80(4)
$Cu^e-Cl-Cu^a$	102.05(4)	104.54(5)
$Cl^f-Cu-Cl^a$	107.76(4)	106.38(5)

Symmetry codes: (a) $1-x$, $-y$, $1-z$; (b) $-0.5+x$, $0.5-y$, $0.5+z$; (c) $1.5-x$, $-0.5+y$, $0.5-z$; (d) $0.5+x$, $0.5-y$, $-0.5+z$; (e) $0.5+x$, $0.5-y$, $0.5+z$; (f) $-0.5+x$, $0.5-y$, $-0.5+z$; (g) $1.5-x$, $0.5+y$, $0.5-z$.

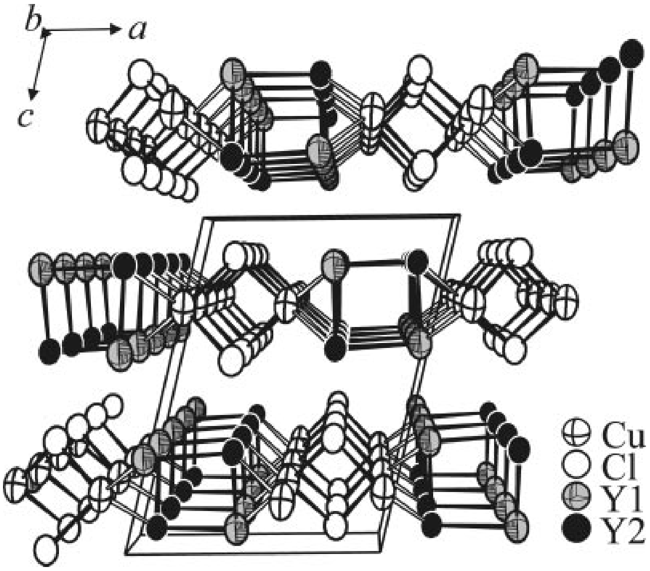

Figure 1 Section of the crystal structure of $CuClSe_xTe_{2-x}$ (x = 0.56; 1.53). Anisotropic displacement parameters represent a probability of 90 %.

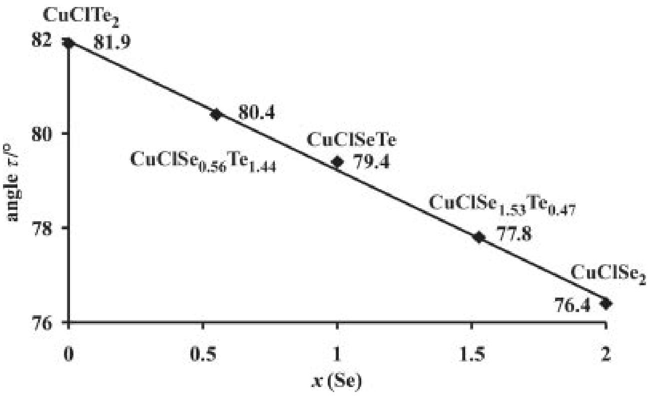

Figure 2 Dependence of the torsion angle τ formed by Cl−Cl edges of neighboured $[CuY1Y2Cl_{2/2}]$ tetrahedra on the substitution parameter x of $CuClSe_xTe_{2-x}$.

atom type for this particular arrangement. A more detailed description of this structure type was already given elsewhere [10, 11].

Tellurium in CuClSeTe and CuClSTe prefers to occupy the position Y2 resulting in a distance d(Te−Cl) to a halide ion of the adjacent layer which is much shorter than the sum of the van der Waals radii. For $CuClY'_xTe_{2-x}$ and $x < 1$ tellurium atoms on the position Y1 are preferably substituted by the heteroatoms S and Se. Thus, a slightly shorter distance to copper is realised, see Figure 3. As a result an almost perfect ordering of the chalcogen atoms is observed. Heteroatomic bonds S/Se−Te result instead of homoatomic bonds Se−Se, S−S or Te−Te. An ordered heteroatomic distribution of the chalcogen atoms in the chains cannot be realized for a 3:1 or 1:3 composition within the given space group symmetry. However, the strong preference of Te for position Y2 results in an almost full occupation of Y1 be Se atoms in $CuClSe_{1.53}Te_{0.47}$, and an amount of about 94% of Te on position Y2 in $CuClSe_{0.56}Te_{1.44}$. Table 5 compares the site occupation factors of Te observable in CuClSTe, CuClSeTe and $CuClSe_xTe_{2-x}$ (x = 0.56, 1.53). The most perfect separation can be observed in case of CuClSTe and $CuClSe_{0.56}Te_{1.44}$ resulting in occupation factors close to the ideal values. Thus the occupation factor of Te on Y2 is 1 and 0.94 for CuClSTe and for $CuClSe_{0.56}Te_{1.44}$, respectively. This clearly indicates the important role of Te−X interactions in this type of compounds. The angle τ spread up by the halide edges of the tetrahedra is dependent on the halide ion, as shown for CuSeTeX (X= Cl, Br, I) [11]. Figure 2 shows the linear dependence of this angle τ on the chalcogen ratio when only one halide ion is regarded.

The small deviations from a perfect ordering of the chalcogen atoms might be explained by entropy reasons during crystal growth. However, the verification of the deviations

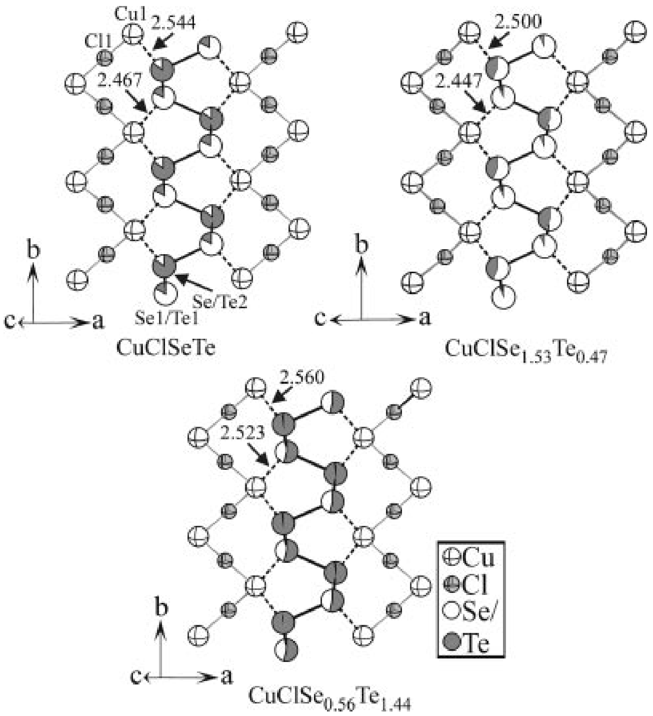

Figure 3 Distribution of Se and Te over the two crystallographically independent positions of the chalcogen chain realised in CuClSeTe (data taken from [11]), $CuClSe_{1.53}Te_{0.47}$, and $CuClSe_{0.56}Te_{1.44}$. Occupancy factors are represented by sectors (white: Se, grey: Te).

Table 5 Site occupation factors of the Y(1) and Y(2) position of CuClSTe, CuClSeTe, $CuClSe_{1.53}Te_{0.47}$, and $CuClSe_{0.56}Te_{1.44}$.

Compound	sof(Te) Y1	sof(Te) Y2	Ref.
CuClSTe	0.060(4)	1.0	[10]
CuClSeTe	0.171(7)	0.851(8)	[11]
$CuClSe_{1.53}Te_{0.47}$	0.073(2)	0.400(2)	
$CuClSe_{0.56}Te_{1.44}$	0.501(3)	0.944(3)	

which were determined by single crystal X-ray diffraction by means of an independent method is highly desirable. Vibrational spectroscopy was chosen, since it is not as sensitive for long range effects as X-ray diffraction.

IR and Raman spectroscopy

An analysis of the interchalcogen stretching modes observed in IR and Raman spectra should help to decide whether the occupation factors of the two positions determined by X-ray techniques are correct. If the minor component is nonetheless distributed over both positions Y1 and Y2, the corresponding vibrations for all combinations, namely Y'−Te, Te−Te, and Y'−Y' should be observed. Therefore spectra were recorded and analysed for a series of seven different copper(I) calcogen halides with the composition CuXYY'. The spectra are displayed in Figures 4 (IR) and 5 (Raman).

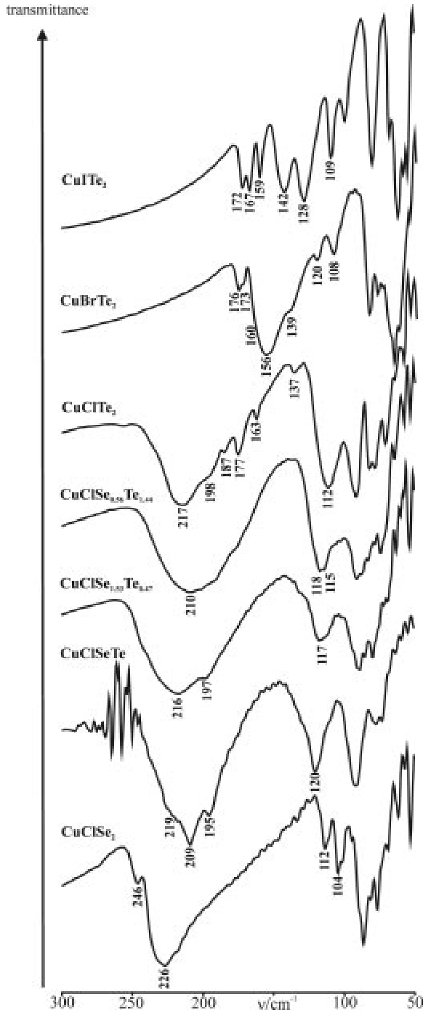

Figure 4 IR spectra of ternary and quaternary copper(I) chalcogen halides.

The IR spectra of CuClSeTe, $CuClSe_2$, and $CuXTe_2$ (X = Cl, Br, I) can be used for a proper assignment of the interchalcogen vibrational bands. In addition, spectra of trigonal Se [21], Se−Te glasses [19, 20], $(CuBr)_2Se_6$, $(CuI)_2Se_6$, [16] and heteronuclear chalcogen rings [17] were used for this purpose. *McWhinnie et al.* observed Te−Te modes of R−Te−Te−R molecules in the region from 187 cm^{-1} to 156 cm^{-1} [18]. In case of $CuITe_2$ one can observe three modes at 172 cm^{-1}, 167 cm^{-1}, and 159 cm^{-1} which are assigned to the chalcogen chain. Modes of the copper(I) iodide chain are localised at 142 cm^{-1} and 128 cm^{-1}. This is in good agreement with the data given for $(CuI)_2Se_6$ [16]. Obviously the bond distances *d*(Cu−X) are much more important for the spectroscopic properties than the 3D-arrangement, e.g. Cu_2X_2 rhomboids vs. chains $^1_\infty$[CuX]. Unfortunately, the modes of the copper(I) halide and of the chalcogen chain overlap in case of $CuBrTe_2$ and $CuClTe_2$. For $CuBrTe_2$ the Cu−X modes are observed at 156 cm^{-1} and 138 cm^{-1} compared to 217 cm^{-1} and 198 cm^{-1} in case of $CuClTe_2$. Despite this overlap modes caused by tellurium

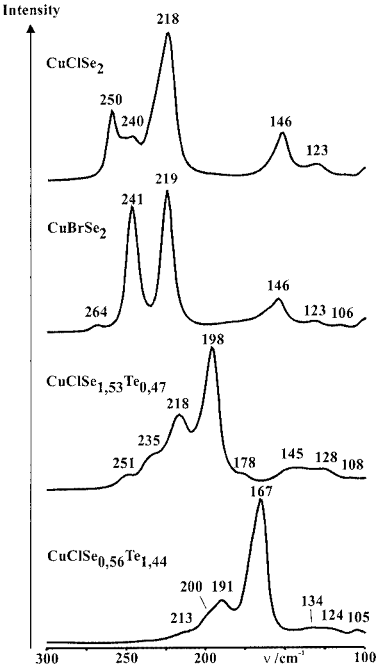

Figure 5 Raman spectra of $CuClSe_2$, $CuBrSe_2$, $CuClSe_{1.53}Te_{0.47}$, and $CuClSe_{0.56}Te_{1.44}$.

can be observed at 176 cm^{-1}, 173 cm^{-1}, and 160 cm^{-1} ($CuBrTe_2$), and at 187 cm^{-1}, 177 cm^{-1}, and 163 cm^{-1} ($CuClTe_2$), respectively.

Modes due to Se−Te bonds can be expected around 205 cm^{-1} (compare to Se−Te glasses [19, 20]). The bands at 209 cm^{-1} and 195 cm^{-1} are due to the Se−Te modes. Se−Se stretching modes can be expected at higher wavenumbers in comparison to the Se−Te modes. In case of $(CuBr)_2Se_6$ and $(CuI)_2Se_6$ modes of Se−Se are observed in the region from 255 cm^{-1} to 242 cm^{-1}. In $CuClSe_2$ one band is found at 246 cm^{-1}. Unfortunately most of the Se−Se and Se−Te modes in $CuClSe_2$ and $CuClSe_xTe_{2-x}$ (x = 0.56, 1, 1.53) are covered by broad Cu−Cl modes. Therefore Raman spectra were recorded to obtain some more information about the bonding situation in the chalcogen substructure.

Raman spectra of copper(I) chalcogen halides are dominated by modes of the chalcogen chains. Copper(I) halide modes are generally weak in the Raman spectra [16]. Se−Se modes can be observed in the region from 250 cm^{-1} to 218 cm^{-1} in good agreement with values calculated for heteroatomic sulphur selenium rings (253 cm^{-1}−209 cm^{-1}) [17], Se_6 (247 cm^{-1} and 221 cm^{-1}) [21] or trigonal Se (237 cm^{-1}, 233 cm^{-1}, and 143 cm^{-1}) [22] (see Figure 4). Comparing homonuclear and heteronuclear compounds (with respect to the chalcogen part) one can observe the occurrence of Se−Te modes at 198 cm^{-1}, and Te−Te modes at 167 cm^{-1}.

Discussion

The modes of the chalcogen chains are supposed to be separated from each other in the spectra due to the mass difference and different force constants. Therefore, one can distinguish between the bands due to homonuclear and heteronuclear bonds in the chalcogen chains of the title compounds. The minority chalcogen atoms can not form homonuclear bonds in case of perfect ordered heteroatomic chalcogen chains.

No homonuclear Se−Se modes are to be observed in the spectrum of $CuClSe_{0.56}Te_{1.44}$. By contrast a weak Se−Se mode occurs in the IR spectra of CuClSeTe. This finding is in good agreement with the distribution of the chalcogen atoms determined by X-ray structure analysis. In this compound the position Y1 is occupied by about 17 % tellurium and the position Y2 is occupied by about 15 % selenium. Thus, a certain number of homonuclear bonds Se−Se can be observed. In the case of $CuClSe_{1.53}Te_{0.47}$ the very weak mode at 178 cm^{-1} is probably due to Te−Te interactions corresponding to 7.3% tellurium localised on the position Y1.

Thus, the distribution of the chalcogen atoms determined by X-ray structure analysis fits the vibrational spectra quite well. However, the question why the chalcogen positions still show a certain mixed occupancy is yet not answered. This finding is certainly due to some entropical effects during sample preparation and the relatively high reaction temperatures. An exchange of the chalcogen atoms upon cooling seems to be not very probable when the chains have once formed and are embedded in the copper halide matrix.

Experimental Section

$CuClSe_{1.53}Te_{0.47}$ and $CuClSe_{0.56}Te_{1.44}$ were prepared by reaction of CuCl (Aldrich, 99.995%), Se (Johnson Matthey, >99.999%), and Te (Heraeus, 99.999%) in evacuated silica ampoules. Stoichiometric mixtures of the starting materials were heated to 500°C for 2 days, and were annealed after homogenisation at 310°C ($CuClSe_{1.53}Te_{0.47}$), and 350°C ($CuClSe_{0.56}Te_{1.44}$), respectively, for two weeks. All products are stable against moisture and air for several months.

The purity of the reaction products was checked by X-ray powder diffraction (SIEMENS D5000, STOE STADIP, $CuK\alpha_1$). Crystals of suitable size were selected for single crystal structure determinations. Intensity data were collected on an IPDS (STOE, Graphite monochromator, Mo K_a, λ = 0.71073 Å), see Table 1 for details.

IR spectra were recorded on an IFS 113V Fourier-Transform-Spectrometer (BRUKER) between 400 cm^{-1} and 50 cm^{-1} with a resolution of ± 2 cm^{-1}. Fine grained samples were run as Nujol mulls suspended on polyethylene plates.

Raman spectra of powdered samples sealed in glass capillaries were recorded on a RFS100/S spectrometer (BRUKER) in a backscattering mode using a Nd:YAG laser with an extinction wavelength of 1064 nm.

Spectral data:

$CuITe_2$IR (Nujol, cm^{-1}): 172 s, 167 s, 159 m, 142 s, 128 vs, 109 m, 99 w, 80 m, 68 m, 62 vs, 58 s, 55 s.

$CuBrTe_2$. IR (Nujol, cm^{-1}): 176 w, 173 w, 160 m,sh, 156 s, 139 m,sh, 120 w, 108 w, 83 s, 77 m, 73 m, 68 s,sh, 66 vs, 62 s, 54 vw.

$CuClTe_2$. IR (Nujol, cm^{-1}): 217 vs, br, 198 s,sh, 187 m, 177 m, 163 w, 137 vw, 112 vs, 93 vs, 84 s, 80 s, 72 m, 66 w, 59 w, 54 vw.

$CuClSe_{0.56}Te_{1.44}$. IR (Nujol, cm^{-1}): 210 vs, br, 118 s, 115 s, 91 vs,br, 75 m, 65 w, 58 vw, 54 vw.
Raman (powder, cm^{-1}): 213 vw, 200 w, 191 m, 167 vs, 134 vw, 124 vw, 105 vw.

CuClSeTe. IR (Nujol, cm^{-1}): 219 s,sh , 212 s,br, 209 vs, 195 s, 120 m, 91 m, 77 w, 73 w.

$CuClSe_{1.53}Te_{0.47}$. IR (Nujol, cm^{-1}): 216 vs,br, 197 s,sh , 117 m,br, 89 s,br, 85 m, 79 s, 71 m, 69 m, 63 w, 60 vw, 57 vw, 53 w.
Raman (powder, cm^{-1}): 251 vw, 235 w, 218 m, 198 vs, 178 vw, 145 w, 128 w, 108 vw.

$CuClSe_2$. IR (Nujol, cm^{-1}): 246 w, 226 vs, br, 112 w, 104 m,102 m, 94 w, 88 s,sh, 86 s, 80 m, 76 m, 68 w, 61 w, 57 vw, 53 w.
Raman (powder, cm^{-1}): 250 m, 240 w, 218 s, 146 w, 123 vw.

$CuBrSe_2$. Raman (powder, cm^{-1}): 264 vw, 241 s, 219 vs, 146 m, 123 vw, 106 vw.

Acknowledgement. Financial support of the Deutsche Forschungsgemeinschaft and the Fonds der Chemischen Industrie is gratefully acknowledged. We thank *Prof. Deiseroth* for continuous support and the facility to use his experimental equipment, and *Prof. Haeuseler, R. Stoetzel* and *J. Hermann* for the measurement of the IR- and Raman-spectra.

References

[1] A. Pfitzner, *Chem. Eur. J.* **2000**, *6*, 1891.
[2] A. Rabenau, H. Rau, G. Rosenstein, *Naturwissenschaften* **1969**, *56*, 137.
[3] W. Milius, A. Rabenau, *Z. Naturforsch.* **1988**, *43 b*, 243.
[4] A. Pfitzner, T. Nilges, *Z. Anorg. Allg. Chem.* **1999**, *625*, 201.
[5] J. Fenner, A. Rabenau, *Acta Crystallogr.* **1976**, *B32*, 3084.
[6] W. Milius, *Z. Naturforsch.***1989**, *44 b*, 990.
[7] W. Milius, *Z. Anorg. Allg. Chem.* **1990**, *586*, 175.
[8] P. M. Carkner, H. M. Haendler, *J. Solid State Chem.* **1976**, *18*, 183.
[9] J. Fenner, A. Rabenau, *Z. Anorg. Allg. Chem.* **1976**, *426*, 7.
[10] A. Pfitzner, S. Zimmerer, *Z. Anorg. Allg. Chem.* **1996**, *622*, 853.
[11] A. Pfitzner, S. Zimmerer, *Z. Anorg. Allg. Chem.* **1995**, *621*, 969.
[12] A. Pfitzner, S. Zimmerer, *Z. Kristallogr.* **1997**, *212*, 203.
[13] C. Näther, M. Wriedt, I. Jeß, *Z. Anorg. Allg. Chem.* **2002**, *628*, 394, and references cited therein.
[14] M. Inui, M. Yao, H. Endo, *J. Phys. Soc. Jpn.* **1988**, *57*, 553.
[15] A. Ikawa, H. Fukutome, *J. Non-Cryst. Solids* **1990**, *117/118*, 328.
[16] J. D. Sarfati, G. R. Burns, *Spectrochim. Acta* **1994**, *50A*, 2125.
[17] R. Laitinen, R. Steudel, E. M. Strauss, *J. Chem. Soc., Dalton Trans.* **1985**, 1869.
[18] W. R. McWhinnie, P. Thavornyutikarn, *J. Organomet. Chem.* **1972**, *35*, 149.
[19] T. Ohsaka, *J. Non-Cryst. Solids* **1975**, *17*, 121.
[20] T. Ohsaka, *J. Non-Cryst. Solids* **1976**, *21*, 23.
[21] N. Nagata, K. Ishibashi, Y. Miyamoto, *Jpn. J. Appl. Phys.* **1981**, *20*, 463.
[22] G. Lucovsky, A. Mooradian, W. Taylor, G. B. Wright, R. C. Keezer, *Solid State Commun.* **1967**, *5*, 113.
[23] G. M. Sheldrick, SHELXL 97, Program for crystal structure refinement, University of Göttingen, 1997.